Superconductor Science and Technology

PAPER • OPEN ACCESS

A numerical method to calculate screening current-dependent self and mutual inductances of REBCO coils

To cite this article: Jeseok Bang *et al* 2023 *Supercond. Sci. Technol.* **36** 085003

OPEN ACCESS
IOP Publishing
Superconductor Science and Technology
Supercond. Sci. Technol. **36** (2023) 085003 (10pp)
https://doi.org/10.1088/1361-6668/acdb9e

A numerical method to calculate screening current-dependent self and mutual inductances of REBCO coils

Jeseok Bang[1,*], Jeonghwan Park[2], Kibum Choi[2], Geonyoung Kim[2] and Seungyong Hahn[2]

[1] National High Magnetic Field Laboratory, Florida State University, Tallahassee, FL 32310, United States of America
[2] Department of Electrical and Computer Engineering, Seoul National University, Seoul 08826, Republic of Korea

E-mail: jbang@asc.magnet.fsu.edu

Received 21 March 2023, revised 16 May 2023
Accepted for publication 5 June 2023
Published 21 June 2023

Abstract
The screening current and its relaxation cause the variation of the self- and mutual inductances of REBCO coils—REBCO is one of the high-temperature superconductors. However, most studies of coil voltage analysis on a REBCO magnet, a stack of coils, have reported simulation results assuming invariant self- and mutual inductances so far. Although the conventional assumption of invariant inductances is still acceptable for fundamental coil voltage analyses, it can cause misleading conclusions due to inductive voltage errors when a precise coil voltage analysis is demanded. Hence, here we report a numerical method to calculate screening-current-dependent self- and mutual inductances of REBCO coils for advanced studies based on a lumped-circuit analysis model. In this work, we aim to investigate the inductance variation due to the screening current with a case study and discuss its effects on the coil voltage. We assume that there is a stack of 12 REBCO single-pancake coils. No transverse current in each coil is considered for simplicity. A numerical simulation of the current density in the magnet is performed, and then the inductances are calculated by considering the spatially non-uniform current density due to the screening current. From this case study, we confirm that the self- and mutual inductances are changed by up to 110% and 30% each. It is also confirmed that the discrepancy is notable at the beginning of the charge while marginal at the end. Finally, we discuss the effect of inductance variation on the quench voltage analysis.

Keywords: coil voltage analysis, high-temperature superconductor magnet, lumped circuit simulation, no-insulation, self and mutual inductances, screening current

(Some figures may appear in colour only in the online journal)

[*] Author to whom any correspondence should be addressed.

1. Introduction

The aftermath of the discovery that observed mechanical damage on a REBCO-coated conductor (hereafter REBCO wire) in a high-temperature superconductor (HTS) insert magnet named 'Little Big Coil' [1] has indeed motivated researchers to investigate screening currents and the consequent effects. So far, it has been revealed that the screening current, the intrinsic induced current to dispel a penetrating magnetic field to every superconducting material, is a dominant source of the created non-uniform current density. Furthermore, through relevant research, it has also been confirmed that the screening current can have pernicious effects on the magnetic force and field distributions, i.e. screening-current-induced stress (SCS) [1] and field (SCF) [2], as they are concentrated at a particular location in a wire. Meanwhile, the pernicious effects are practically mitigated by making a multi-filament structure; therefore, some selected superconductor materials, e.g. Nb_3Sn and Bi2212, are resolved from the relevant issue by making multi-filament wire. However, mainly due to the material properties, the technique is impractical for REBCO wires. As a result, the screening current in REBCO wire has become a key concern when building an HTS magnet wound with REBCO wire.

According to the relevant research of the screening current in an HTS coil or magnet wound with REBCO wire (hereafter REBCO coil or magnet), it is widely reported that the screening current causes non-uniform current density, usually concentrated at both edges of a REBCO wire, and thus induces a change in the magnetic flux and magnetic force distribution. Fortunately, the changes can be measured as physical quantities, i.e. magnetic field, voltage, and strain, using an instrumentation system. Among them, the quantities of magnetic field and strain changed by the screening current, i.e. SCF [2–8] and SCS [9–13], have been actively studied. However, there is a need for additional research on the magnetic inductive component change between REBCO coils and thus coil voltage behavior. As a representative example, it is widely agreed that the self- and mutual inductances of multiple REBCO coils in a magnet are changed depending on the operating current due to the screening current and its relaxation. However, most studies adopting the lumped-circuit model have provided calculation results that assume invariant inductances, although a previous study has raised the relevant issue of transport current-dependent coil inductance [14]. This may be because the inductance calculation method that considers the screening current has not yet been developed.

Hence, this paper aims to propose an inductance calculation method with the screening current considered, investigates inductance variation due to the screening current via a case study, and discusses its effect on coil voltage. This study employs a stack of 12 REBCO single-pancake (SP) coils. For simplicity, no transverse current in each coil is assumed. In addition, the field-dependent critical current is not considered. Meanwhile, we consider the various matrices in the wire material, including REBCO, as one bulk and assume its permeability to be the vacuum permeability (μ_0). Then, a numerical simulation of the current density in the magnet is performed, and the inductances are calculated by considering the spatially non-uniform and temporally non-linear current densities due to the screening current. Limited to this case study, we confirm that the self- and mutual inductances are changed up to 110% and 30% each. It is also confirmed that the discrepancy is notable at the beginning of the charge while marginal at the end. Finally, we will discuss the effect of inductance variation on the quench voltage analysis.

2. Method

A REBCO magnet is a spatially non-uniform and temporally non-linear current density system due to a screening current. Hence, it is barely possible to employ the conventional methods of self- and mutual inductance calculation, which were developed based on the direct integration of Neumann formulae or a magnetic vector potential assuming the linear and homogeneous current density system [15–17]. In this work, we thus propose a numerical technique to calculate the inductance using the finite element method (FEM) simulation approach based on the so-called *energy method*.

The current density of a REBCO magnet with the screening current included can be obtained using time-dependent FEM simulation, as shown in figure 1. It presents an example of the non-uniform current density in two arbitrarily selected coils (REBCO-Coil1 and Coil2) in a magnet, i.e. a stack of multiple REBCO coils. Here, all the coils in a magnet are assumed to be connected in series and charged up to a designated current (I) at a certain time (t) with a constant ramp rate. Using the FEM simulation results, the total magnetic stored energy of the two REBCO coils (E_m) is calculated using equation (1):

$$E_m = E_{m1} + E_{m2} + E_{m1,2}, \tag{1}$$

where E_{m1}, E_{m2}, and $E_{m1,2}$ are magnetic stored energies induced by REBCO-Coil1 itself, REBCO-Coil2 itself, and REBCO-Coil1 and Coil2 magnetic coupling, respectively. Here, E_{m1}, E_{m2}, and $E_{m1,2}$ are calculated using equations (2)–(6) in reference to figure 2:

$$E_{m1} = \frac{\mu_0}{2}\int_V \mathbf{H}_1 \cdot \mathbf{H}_1 \, \mathrm{d}v, \tag{2}$$

$$E_{m2} = \frac{\mu_0}{2}\int_V \mathbf{H}_2 \cdot \mathbf{H}_2 \, \mathrm{d}v, \tag{3}$$

$$E_{1,2}^{+} = \frac{\mu_0}{2}\int_V (\mathbf{H}_1 + \mathbf{H}_2) \cdot (\mathbf{H}_1 + \mathbf{H}_2) \, \mathrm{d}v, \tag{4}$$

$$E_{1,2}^{-} = \frac{\mu_0}{2}\int_V (-\mathbf{H}_1 + \mathbf{H}_2) \cdot (-\mathbf{H}_1 + \mathbf{H}_2) \, \mathrm{d}v, \tag{5}$$

$$E_{m1,2} = \frac{E_{1,2}^{+} - E_{1,2}^{-}}{2}, \tag{6}$$

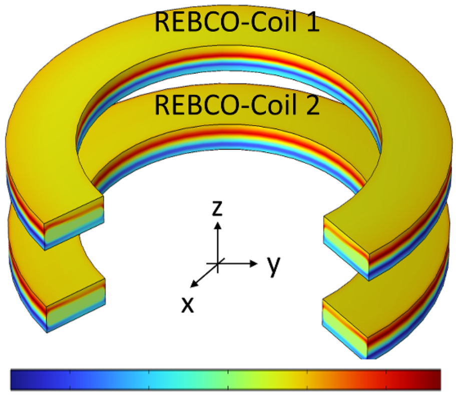

Figure 1. An example of current density calculation results in two REBCO coils with the screening current included.

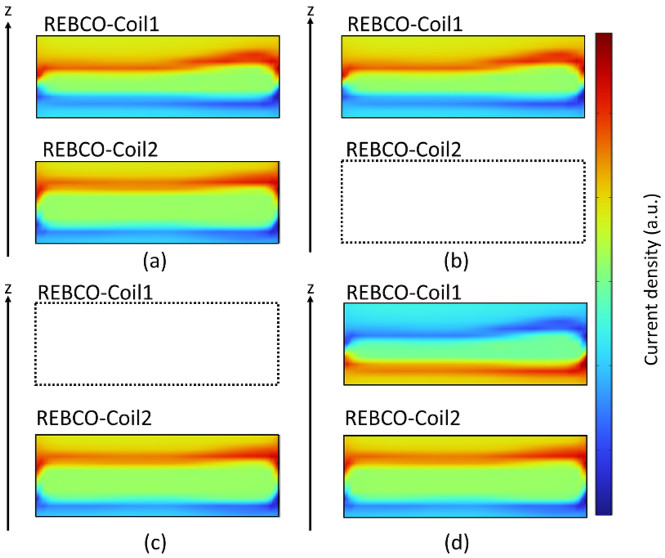

Figure 2. The current density setup to calculate magnetic stored energies in the axisymmetric domain: (a) for $E^{+}_{1,2}$, (b) for E_{m1}, (c) for E_{m2}, and (d) for $E^{-}_{1,2}$.

where $\mathbf{H}_1$ and $\mathbf{H}_2$ are induced magnetic fields by the REBCO-Coil1 current density ($J_{\phi,1}$), and REBCO-Coil2 current density ($J_{\phi,2}$) when I flows in both coils. Note that $-\mathbf{H}_1$ is calculated using $-J_{\phi,1}$ in Coil1. This has reciprocity as we use $-J_{\phi,2}$ in Coil2.

Meanwhile, the relationship between energy, magnetic flux, and self- and mutual inductances should be defined differently from the conventional relationship assuming the linear and homogeneous current density system. The results are summarized below:

$$L_1(I) = \lim_{\Delta I \to 0} \frac{\lambda_1(I+\Delta I) - \lambda_1(I)}{\Delta I} = \frac{\partial \lambda_1}{\partial I} \neq \frac{\lambda_1}{I}, \quad (7)$$

$$L_2(I) = \lim_{\Delta I \to 0} \frac{\lambda_2(I+\Delta I) - \lambda_2(I)}{\Delta I} = \frac{\partial \lambda_2}{\partial I} \neq \frac{\lambda_2}{I}, \quad (8)$$

$$M_{1,2}(I) = \lim_{\Delta I \to 0} \frac{\lambda_{1,2}(I+\Delta I) - \lambda_{1,2}(I)}{\Delta I} = \frac{\partial \lambda_{1,2}}{\partial I} \neq \frac{\lambda_{1,2}}{I}, \quad (9)$$

$$M_{2,1}(I) = \lim_{\Delta I \to 0} \frac{\lambda_{2,1}(I+\Delta I) - \lambda_{2,1}(I)}{\Delta I} = \frac{\partial \lambda_{2,1}}{\partial I} \neq \frac{\lambda_{2,1}}{I}, \quad (10)$$

$$\lambda_1(I) = \lim_{\Delta I \to 0} \frac{E_{m1}(I+\Delta I) - E_{m1}(I)}{\Delta I} = \frac{\partial E_{m1}(I)}{\partial I} \neq \frac{1}{2} L_1 I^2, \quad (11)$$

$$\lambda_2(I) = \lim_{\Delta I \to 0} \frac{E_{m2}(I+\Delta I) - E_{m2}(I)}{\Delta I} = \frac{\partial E_{m2}(I)}{\partial I} \neq \frac{1}{2} L_2 I^2, \quad (12)$$

$$\lambda_{1,2}(I) = \lim_{\Delta I \to 0} \frac{E_{m1,2}(I+\Delta I) - E_{m1,2}(I)}{\Delta I} = \frac{\partial E_{m1,2}(I)}{\partial I} \neq \frac{1}{2} M_{1,2} I^2, \quad (13)$$

$$\lambda_{2,1}(I) = \lim_{\Delta I \to 0} \frac{E_{m2,1}(I+\Delta I) - E_{m2,1}(I)}{\Delta I} = \frac{\partial E_{m2,1}(I)}{\partial I} \neq \frac{1}{2} M_{2,1} I^2. \quad (14)$$

Here, L, M, λ, and I present, respectively, self-inductance, mutual inductance, flux linkage, and the current in coils. The subscripts indicate which coils are the sources of magnetic flux or flux linkage. Here, ΔI is the current increment corresponding to the time increment (Δt). The last term of equations (7)–(14) is the definition of the conventional relationship.

So far, we have proposed and explained the inductance calculation method based on the energy method with two arbitrarily selected REBCO coils in a magnet. From now on, the entire computation process of the proposed method for a stack of N_{coil} REBCO module coils is discussed, by considering the time-dependent FEM simulation; note that the module coil can be in the shape of an SP, double-pancake, etc. The first stage is to calculate the current density by considering all the N_{coil} REBCO module coils and magnet operation scenario. This step is performed with time-dependent FEM simulation, adopting various electromagnetic formulation approaches, e.g. H-formulation, T-A formulation, and others [18–23]. One thing to note is that the time step for the time-dependent simulation should be appropriately divided to calculate self- and mutual inductances accurately. Here, it is recommended to set the current increment according to the time step not exceeding a maximum of 1 A. The second stage is to select two module coils in the given coil stack and to calculate magnetic stored energies caused by the selected coils by considering every time step. If the number of time steps for the time-dependent FEM simulation is N_{step}, the number of computations demanded in this second stage (N_{comp}) is described with equation (15):

$$N_{\text{comp}} = \frac{N_{\text{step}} \times \binom{N_{\text{coil}}}{2} \times 4}{2}. \quad (15)$$

The reason for multiplying by 4 and dividing by 2 is that a total of four computation times are necessary for magnetic energy calculation, and the matrix consisting of self- and mutual inductances is symmetric. The last stage is to derive the self- and mutual inductances of all the N_{coil} REBCO module coils at the ith time step and the corresponding current, using the calculation results of magnetic stored energies at $(i-1)$th, ith, $(i+1)$th time steps.

Table 1. The key parameters of a solenoid magnet.

Magnet parameters	Unit	
Conductor width, w	(mm)	4.10
Conductor thickness, th	(mm)	0.12
Inner radius, a_1	(mm)	50
Outer radius, a_2	(mm)	59.36
The number of module coils		12
The number of turns		80
Operating current, I_{op}	(A)	100
Critical current, I_{c}	(A)	100
Critical current density, J_{c}	(A mm^{-2})	200
Index value for power law		21
Ramp rate	(A s^{-1})	0.01
Time step for simulation (Δt)	(s)	1

3. Results and discussion

Table 1 presents the key parameters of a REBCO solenoid magnet chosen for a case study [24]. The magnet is a stack of 12 module coils, and each module coil is in the shape of an SP. In this case study, we utilized the FEM simulation with H-formulation by adopting edge-element and domain homogenization techniques [18, 19]. A power-law model [25] was used to consider the REBCO material properties of resistivity. The field-dependent critical current properties were not considered. It was assumed that the magnet is charged up to its operating current of 100 A—it is the same value as its critical current—with a constant ramp rate of 0.01 A s^{-1}. The calculation results of the current density with the screening current included were saved at every time step; this time-step setup corresponds to 0.01 A of coil current.

Figure 3 presents the calculation results for the non-uniform current density in REBCO coils with the screening current included. Here, ϵ is the ratio of the operating current to the critical current ($\frac{I_{\text{op}}}{I_{\text{c}}}$). It is found that the current density in each coil is concentrated at both edges of each coil at the beginning of the charge, but the distribution relaxes and penetrates toward the center of each coil, depending on ϵ. Figure 4 shows the total sum of self- and mutual inductances according to the current density provided in figure 3 at the magnet level, while figure 4 is at the module coil level; the lower half section of the magnet is selected to display representatively, by considering the symmetric properties of the inductance matrix. They provide three sets of calculation results: REF, UNI, and SC. Graphs named 'REF' show the calculation results based on the direct integration of Neumann formulae and assuming uniform current density, which is the reference result to compare with other calculation results. Graphs named 'UNI' show the calculation results based on FEM simulation with the screening current excluded while applying the proposed inductance calculation method. Note that this simulation can be easily performed with an electromagnetic simulation module embedded in commercial numerical simulation software, without using electromagnetic formulation approaches. Graphs named 'SC'

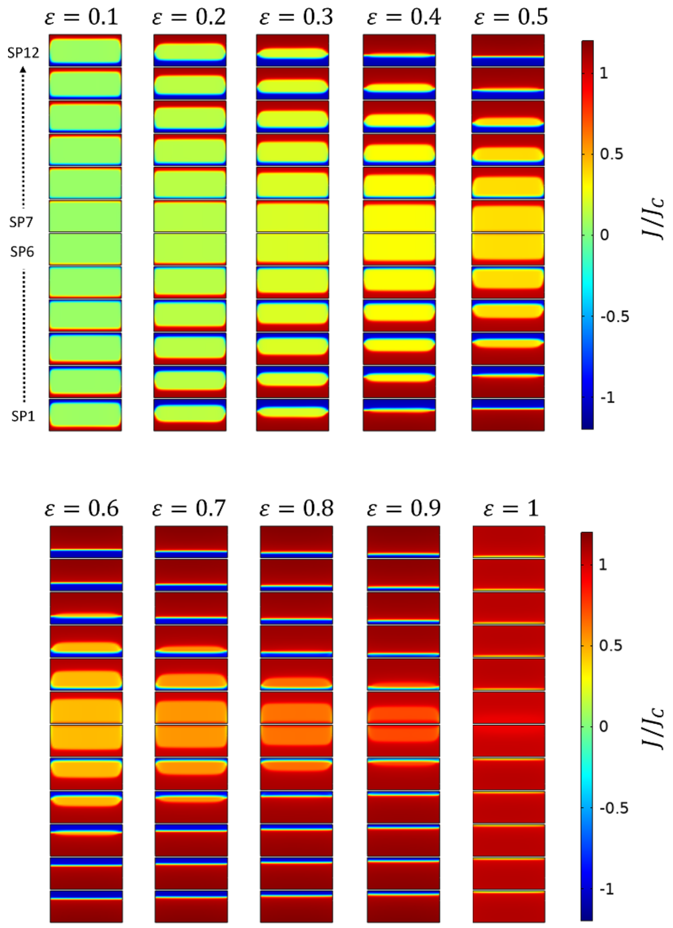

Figure 3. The calculation results of non-uniform current density in a REBCO magnet with the screening current considered (displayed in the coil's cross-section domain).

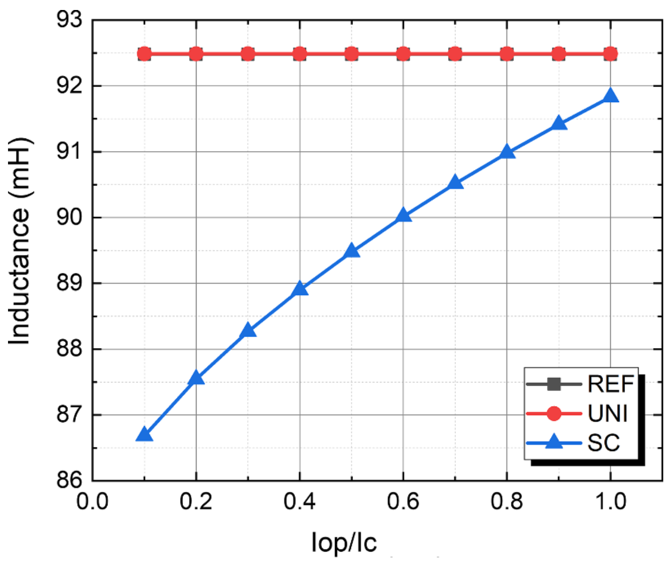

Figure 4. Magnet inductance: the sum of the self- and mutual inductances between all individual coils.

show the calculation results based on FEM simulation with the screening current included and the proposed method used. According to the current density variation depending on ϵ, the non-linear inductance variation between REBCO coils is confirmed. It is also confirmed that the notable variation shown in figures 4 and 5 tends to increase, except for two coils at the

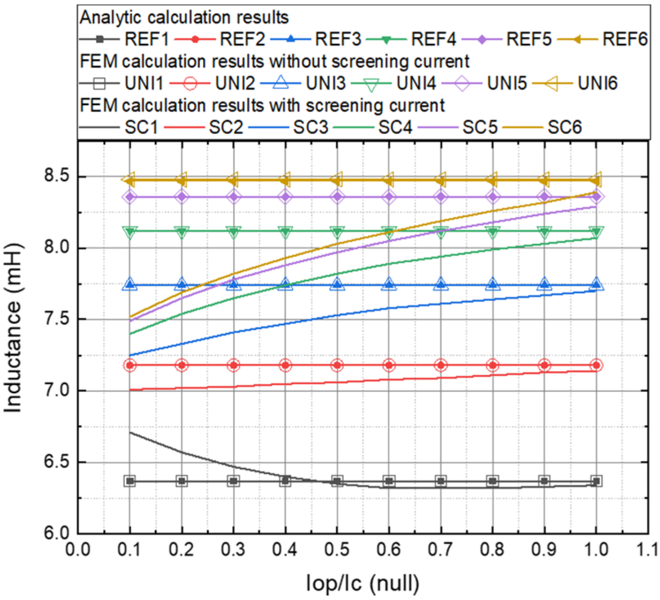

Figure 5. The coil inductances of SP1–6. Coil inductance of a coil in a REBCO magnet (a stack of REBCO coils) means the sum of the self-inductance of a given coil and mutual inductances between a given coil and the other coils.

top and bottom of the magnet, while it tends to decrease at the top and bottom. Meanwhile, it is suggested that the proposed method is validated by the comparison results between the graphs named 'REF' and 'UNI'.

Figures 6 and 7 provide the self- and mutual inductance calculation results in detail and the errors between the calculated results. Here, the error was calculated using:

$$\text{error }[\%] = \frac{M_{i,j}^{\text{SC}} - M_{i,j}^{\text{REF}}}{M_{i,j}^{\text{REF}}} \times 100, \tag{16}$$

where $M_{i,j}^{\text{SC}}$ and $M_{i,j}^{\text{REF}}$ stand for the mutual inductance between the *i*th module coil and the *j*th module coil by considering the non-uniform current density due to the screening current, and that considering the uniform current density. As a result, we confirm that the self- and mutual inductances are changed by up to 110% and 30% each (limited to this case study).

From this study investigating the self- and mutual inductances depending on the operating current and screening current, we have found that the conventional lumped-circuit model that considers invariant inductances may have limitations when precisely simulating the coil voltage. Hence, in this paper, we suggest a modified lumped circuit and the corresponding governing equation. To investigate the general case of solenoid REBCO coils or magnets, we consider not only the azimuthal current path but also the radial current path that can be induced by the so-called no-insulation (NI) feature. Figure 8 presents conventional and modified models of the most basic example, i.e. one coil or magnet. The key difference between the governing equations of the two models is the voltage

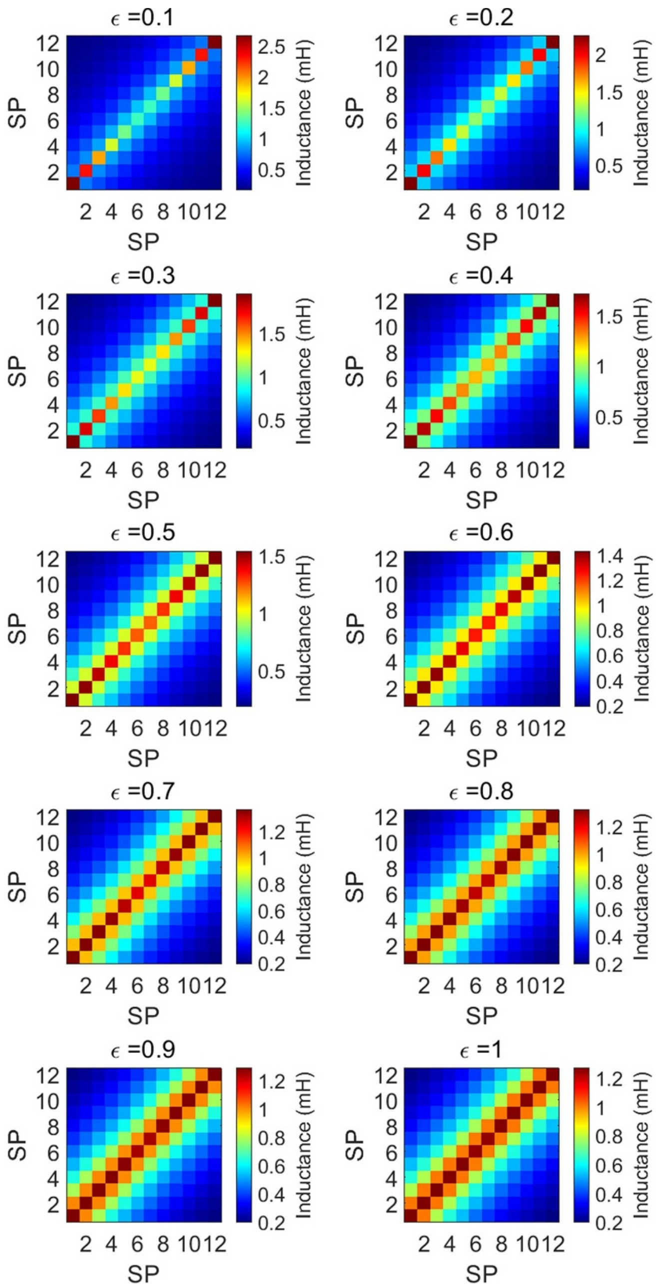

Figure 6. The numerical simulation results of the time-varying 'equivalent' inductance of each module coil in the given REBCO magnet according to the operating current.

equation: equation (17) for figure 8(a), and equation (18) for figure 8(b),

$$V = L_{\text{conv}} \frac{\mathrm{d}I_\phi}{\mathrm{d}t} + R_{\text{sc}} I_\phi, \tag{17}$$

$$V^* = \delta V_\lambda \left(= \frac{\mathrm{d}\lambda}{\mathrm{d}t} \right) + R_{\text{sc}} I_\phi, \tag{18}$$

where V, V^*, L_{conv}, I_ϕ, I_r λ, R_{sc}, and R_{c} are, respectively, voltage without consideration of the screening current, voltage

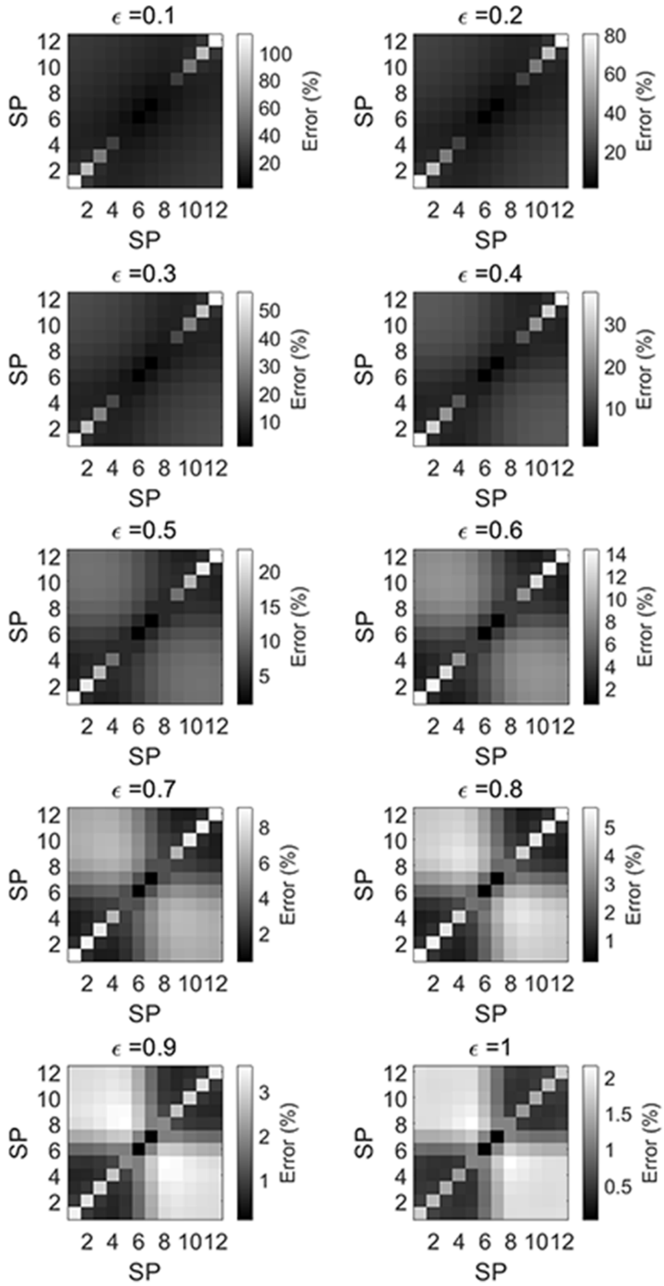

Figure 7. Self- and mutual-inductance errors between the calculation results, with and without considering the screening current. It is calculated using equation (16).

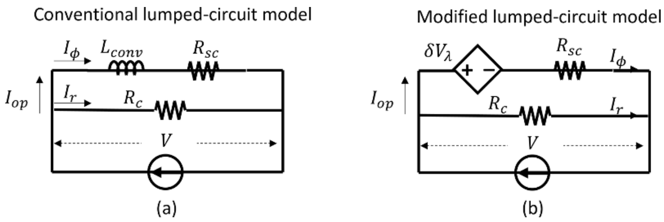

Figure 8. The lumped-circuit models of a REBCO module coil or magnet: (a) the conventional model; (b) the modified model (proposed).

with consideration of the screening current, inductance without consideration of the screening current, the current flowing in REBCO wire, the current flowing in the contact layers between adjacent REBCO wires, current-dependent non-linear magnetic flux linkage caused by a REBCO coil or magnet, REBCO resistivity—in this study, the power-law

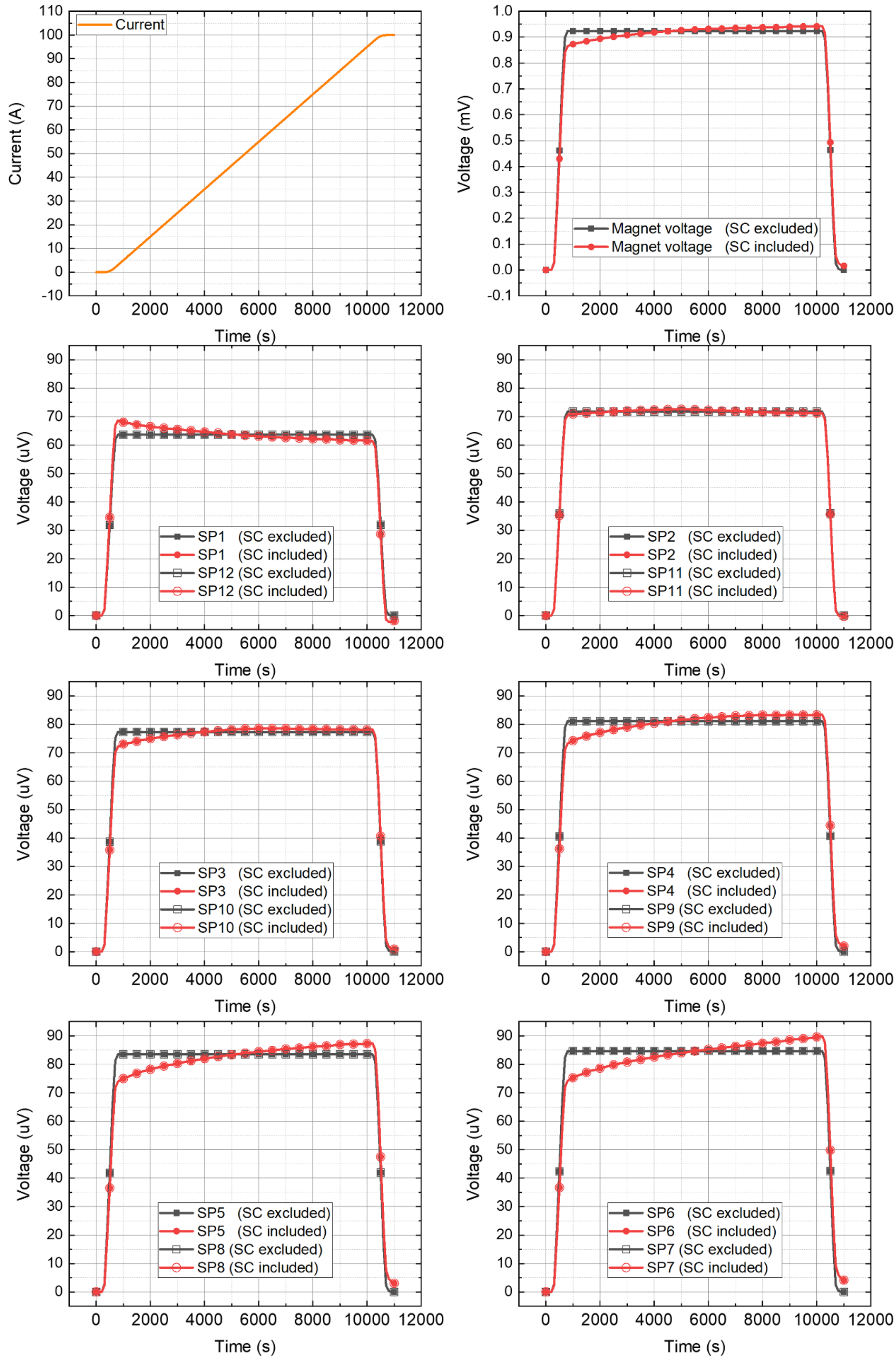

Figure 9. Comparisons between the calculation results with equation (17) and those with equation (18): black lines and red lines, respectively. The current, inductive voltage of the magnet, and inductive voltage of each coil are considered. A 'smoothing' technique is applied at the beginning and end of the current charging so that the second derivative of the current profile is continuous.

model is considered—and the resistance along the contact layers.

We have applied this proposed circuit model, figure 8(b), to the case study, and the results are shown in figure 9. We built a circuit network consisting of 12 modified lumped-circuit models connected in series. Here, $R_c = \infty$ was assumed so that the NI feature was not considered for simplicity. The circuit simulation was performed to investigate voltage behavior differences when the screening current is considered and when it is not. In figure 9, the black lines with symbols are the calculated results considering equation (17) and figure 8(a), and the red lines with symbols are the calculated results considering equation (18) and figure 8(b). With this study, we can conclude that the inductive voltage agrees well with the inductance change shown in figure 5; for instance, the top and bottom coil (SP1&12) voltages decrease as the operating current increases, while the central coil (SP6&7) voltages increase as the operating current increases.

Finally, we would like to discuss the inductance variation effect on the quench voltage simulation of an NI REBCO magnet using the lumped-circuit simulation model. A stack of NI REBCO coils becomes a multiple-current system during the coil quench since the transverse current flowing along the turn-to-turn contact surface of each coil can no longer be negligible. If the inductive voltage depending on self- and mutual inductance variation is marginal (for instance, if the magnet is charged with a slow ramp rate), the proposed method may still be valid. However, assuming that each coil's transport current changes drastically like a quench, the screening-current-dependent inductance should be calculated using our proposed method together with an incremental energy method [26]. Revisiting the relevant literature, numerous studies investigating voltage behavior during quench have been reported so far. However, it is commonly concluded that the simulation results agree reasonably well with the measurement results but are somewhat different from the measured results. Based on this investigation study, we suggest that the voltage difference between the simulation and measurement results is a result of the fact that the invariant inductance has been used.

4. Conclusion

This work has proposed a numerical method to calculate the self- and mutual inductances of coils in a REBCO magnet by varying the screening current and a modified circuit model that considers inductive voltage variation by the screening current. A case study was performed to validate the proposed inductance calculation method and to discuss the effects of the variation of self- and mutual inductances on coil voltage analysis. An additional study with a modified circuit model was performed to investigate the effect of screening-current variation and the consequent inductance change on coil voltage. From these studies, it was confirmed that the self- and mutual inductances of REBCO coils can be significantly changed during a charging operation. Furthermore, it was deduced that the inductance change of each coil and the consequent inductive voltage change may be indicative of estimating the degree of non-uniform current density in each coil, as calculated from the aspect in which the inductance changes depending on the coil location. Finally, we suggest a key concern regarding the comparison results and some discrepancies in the quench voltage analysis between the measurement and simulation: the fact that the self- and mutual inductance variations might be one of the dominant causes of the difference. We hope this work motivates HTS magnet researchers to develop advanced quench voltage simulations.

Data availability statement

All data that support the findings of this study are included within the article (and any supplementary files).

Acknowledgments

A portion of this work was performed at the National High Magnetic Field Laboratory, which is supported by the National Science Foundation Cooperative Agreement No. DMR-2128556 and the State of Florida. This work is also supported by the Office of Fusion Energy Sciences Grant DE-SC0022011.

ORCID iDs

Jeseok Bang https://orcid.org/0000-0002-4761-6334
Jeonghwan Park https://orcid.org/0000-0002-7756-7844
Geonyoung Kim https://orcid.org/0000-0003-4785-3804
Seungyong Hahn https://orcid.org/0000-0002-4511-4162

References

[1] Hahn S *et al* 2019 *Nature* **570** 496–9
[2] Hahn S-Y, Bascuñán J, Kim W, Bobrov E S, Lee H and Iwasa Y 2008 *IEEE Trans. Appl. Supercond.* **18** 856–9
[3] Ahn M C, Yagai T, Hahn S, Ando R, Bascunan J and Iwasa Y 2009 *IEEE Trans. Appl. Supercond.* **19** 2269–72
[4] Jang J Y, Hwang Y J, Han J H, Ahn M, Yang H, Hahn S, Bang J and Lee S 2020 *Supercond. Sci. Technol.* **33** 025005
[5] Yanagisawa Y *et al* 2010 *IEEE Trans. Appl. Supercond.* **20** 744–7
[6] Yanagisawa Y *et al* 2010 *IEEE Trans. Appl. Supercond.* **21** 1640–3
[7] Yang D, Kim K, Choi Y, Kwon O, Park Y and Lee H 2013 *Supercond. Sci. Technol.* **26** 105025
[8] Dilasser G, Fazilleau P and Tixador P 2016 *IEEE Trans. Appl. Supercond.* **27** 1–4
[9] Li Y, Park D, Lee W, Choi Y, Tanaka H, Bascuñàn J and Iwasa Y 2020 *IEEE Trans. Appl. Supercond.* **30** 1–5
[10] Yan Y, Li Y and Qu T 2021 *Supercond. Sci. Technol.* **35** 014003
[11] Yan Y, Song P, Xin C, Guan M, Li Y, Liu H and Qu T 2021 *Supercond. Sci. Technol.* **34** 085012
[12] Kolb-Bond D, Bird M, Dixon I, Painter T, Lu J, Kim K, Kim K, Walsh R and Grilli F 2021 *Supercond. Sci. Technol.* **34** 095004
[13] Ueda H, Maeda H, Suetomi Y and Yanagisawa Y 2022 *Supercond. Sci. Technol.* **35** 054001
[14] Chen S, Gu C, Li Y, Lai L, Qu T, Hu N, Song M, Zou S and Yue Y 2019 *IEEE Trans. Appl. Supercond.* **29** 1–4
[15] Rosa E B and Grover F W 1948 *Formulas and Tables for the Calculation of Mutual and Self-Inductance* vol 169 (Washington, DC: US Government Printing Office)
[16] Garrett M W 1963 *J. Appl. Phys.* **34** 2567–73
[17] Hoer C and Love C 1965 *J. Res. Natl Bur. Stand.* C **69** 127–37

[18] Brambilla R, Grilli F and Martini L 2006 *Supercond. Sci. Technol.* **20** 16
[19] Zermeno V M, Abrahamsen A B, Mijatovic N, Jensen B B and Sørensen M P 2013 *J. Appl. Phys.* **114** 173901
[20] Mykola S and Fedor G 2019 *Supercond. Sci. Technol.* **32** 115001
[21] Bortot L *et al* 2020 *IEEE Trans. Appl. Supercond.* **30** 1–11
[22] Zhang K, Hellmann S, Calvi M and Schmidt T 2020 *IEEE Trans. Appl. Supercond.* **30** 1–5
[23] Oh D K 2022 *IEEE Trans. Appl. Supercond.* **32** 1–8
[24] Bang J *et al* 2020 *IEEE Trans. Appl. Supercond.* **30** 1–5
[25] Rhyner J 1993 *Physica* C **212** 292–300
[26] Gyimesi M and Ostergaard D 1999 *IEEE Trans. Magn.* **35** 1119–22